

LONGITUDINAL TOMOGRAPHY IN A SCALING FFA

D. J. Kelliher*, J.-B. Lagrange, S. Machida, C. R. Prior, C. T. Rogers,
STFC Rutherford Appleton Laboratory, UK
Y. Ishi, Y. Kuriyama, H. Okita, T. Uesugi,

Kyoto University Institute of Integrated Radiation and Nuclear Science[†], Japan,
S. L. Sheehy, University of Oxford, Oxford, UK & University of Melbourne, Australia,
C. Brown, Brunel University, UK and STFC Rutherford Appleton Laboratory, UK.

Abstract

In a synchrotron the rate of acceleration is limited by the ramp rate of the bending field. There is no such constraint in a Fixed Field alternating gradient Accelerator (FFA), allowing a much higher repetition rate and novel modes of operation such as beam stacking. It is of interest to obtain a picture of the longitudinal phase space from experimental data in order to diagnose the response of the beam to various RF programmes. Longitudinal tomography, already well established in synchrotrons, involves reconstructing the phase space using bunch monitor data obtained for a sufficient number of turns in a synchrotron oscillation. Here we reconstruct the longitudinal phase space using data from the 150 MeV scaling FFA at KURNS, Osaka, Japan.

INTRODUCTION

Bunch monitor data, when measured turn-by-turn, provides projections of the longitudinal distribution $f(\phi, \delta)$, where δ is the momentum, onto the phase axis ϕ . Longitudinal tomography uses back projection to reconstruct the phase space, given data from a sufficient number of turns (apart from the case of an equilibrium distribution [1], at least half a synchrotron period is required). A well established tomography code developed at CERN for use in synchrotrons [2,3] employs an algebraic iterative algorithm in conjunction with tracking to allow for non-rigid synchrotron oscillations. This code, and others that apply a similar algorithm, have been widely used [4–7]. However, longitudinal tomography has not been performed using data from a FFA up to now.

Here we show how the CERN tomography code can be used in a scaling FFA. In these machines the orbit moves with momentum to follow the direction of increasing vertical field but the tunes are held constant by ensuring the normalised gradient is fixed. To meet this condition, each magnet has radial profile $B = B_0(r/r_0)^k$ where B_0 is the vertical field at reference radius r_0 and k is the constant field index [8]. In the radial scaling FFA at least one defocusing (reverse bend) magnet per cell is added for vertical tune stability. To maintain a bunched beam throughout acceleration, the scaling FFA utilises phase stability just like a synchrotron.

* David.Kelliher@stfc.ac.uk

[†] KURNS

TOMOGRAPHY CODE

Algorithm

Starting with a set of profile measurements $b(\phi, m)$, where m is the turn number, the reconstruction seeks to find the phase space distribution $x(\phi, \delta)$ such that $A[\phi, \delta, m]x = b$. In order to calculate the operator A , test particles in cells covering the height and phase extent of the bucket, are tracked according to the longitudinal equations of motion (the self-field voltage can be added if desired). In the absence of space charge, the phase and energy (ϕ, E) of test particle i at turn m is incremented as follows

$$\Delta\phi_{i,m+1} = \Delta\phi_{i,m} - 2\pi h \left(\frac{\eta_{0,m}\Delta E_{i,m}}{\beta_{0,m}^2 E_{0,m}} \right) \quad (1)$$

$$\Delta E_{i,m+1} = \Delta E_{i,m} + q[V_{\text{rf},m+1}(\phi_{0,m+1} + \Delta\phi_{i,m+1}) - V_{\text{rf},m+1}(\phi_{0,m+1})] \quad (2)$$

where $h, \eta, \beta, V_{\text{rf}}$ refer to harmonic number, phase slip, the relativistic quantity and the RF voltage. The zero subscript refers to the synchronous particle. For each turn, the distribution of test particles is projected into bins along the phase axis by summing each column of cells. The operator A is calculated so allowing the back projection of each profile bin for each turn, resulting in a first pass calculation of the distribution (see [4] for more details). A discrepancy parameter d is then calculated which quantifies the difference between the forward projected distribution and the turn-by-turn measurements:

$$d = \sqrt{\frac{1}{M} \sum_j^M (e_j - r_j)^2} \quad (3)$$

where e_j and r_j are the measured and reconstructed contents of the j -th bin and M is the total number of bins involved in the reconstruction. The code then repeats the backward and forward projection steps until the discrepancy converges [2].

FFA Case

In this paper the CERN tomography code is used for the FFA case. The code assumes a fixed radius r when calculating the revolution frequency $\omega_{0,m}$ via

$$\omega_{0,m} = \frac{\beta_{0,m}c}{r}. \quad (4)$$

Time is then converted to phase as required by the equations of motion (Eqns. 1 and 2). Here a fixed r is assumed by

Content from this work may be used under the terms of the CC BY 3.0 licence (© 2019). Any distribution of this work must maintain attribution to the author(s), title of the work, publisher, and DOI

taking the average RF frequency for the time period when the data was taken

$$r = \frac{h\beta_{0,m}c}{\langle\omega_{rf}\rangle}. \quad (5)$$

This is an approximation as the radius in a FFA increases with momentum. However, assuming a fixed r when the number of turns used in the analysis is limited to a synchrotron period is acceptable in a typical scaling FFA.

In order for the phase slip to be calculated, the momentum compaction factor α_p should be supplied. Since the radius varies with $r \propto p^{\frac{1}{k+1}}$ it follows

$$\alpha_p = \frac{dr/r}{dp/p} = \frac{1}{k+1}. \quad (6)$$

The design field index is assumed in this analysis — in future a value obtained from measurements [9] may be used.

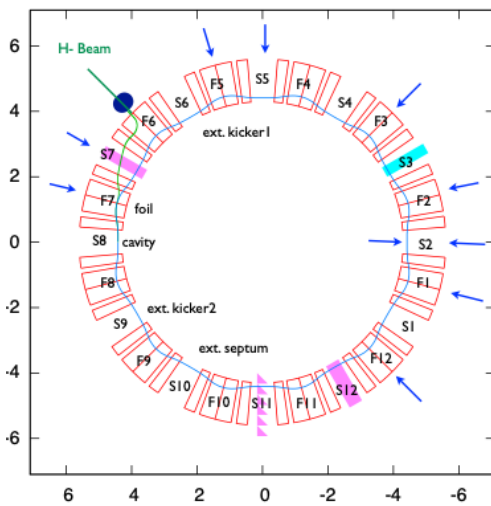


Figure 1: Schematic of the KURNS 150 MeV FFA ring. Blue arrows show where radial probe ports are located. The RF cavity is in cell 8 and there are bunch monitors in cells 7, 11 and 12 (pink). The closed orbit at injection is also shown.

THE EXPERIMENT

KURNS 150 MeV FFA

The tomography code was tested using data taken on the 150 MeV proton ring at KURNS, Osaka [10]. 11 MeV H^- ions from a linac are stripped by a foil. The resulting protons are accelerated in the 12 cell, regular scaling DFD lattice by a single broadband magnetic alloy (MA) cavity typically operating at 4 kV. The radius at injection is about 4.5 m and the nominal field index 7.6. The bunch is detected at several bunch monitors distributed around the ring — for this study we use the monitor 4 cells downstream of the RF cavity as depicted in Fig. 1.

The broadband cavity and the fixed field of the FFA allows great flexibility in setting the RF programme. This is done by specifying the RF waveform for the entire cycle using an Arbitrary Waveform Generator (AWG). The turn-by-turn energy gain is dictated by the rate of change of RF frequency.

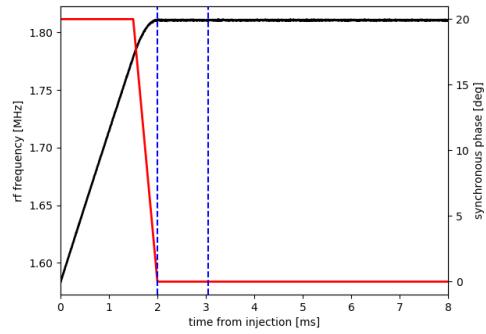


Figure 2: Example of the RF frequency pattern applied in the experiment (black line). The nominal 20 degree synchronous phase is reduced to zero in the interval 1.5 ms to 2 ms (red line). The dashed blue lines correspond to the time interval shown in Fig. 4.

Determining the RF Phase

The delay between the RF waveform and the bunch monitor signal must be established in order to know the absolute phase. The delay is made up of the intervening time of flight and any difference in cable length connecting the gap voltage monitor and bunch monitor to the scope in the control room. Here we make use of the left/right symmetry of the stationary bucket to search for the synchronous phase in the bunch monitor data.

In an experiment to establish the delay, the bunch is first accelerated for about 1.5 ms to ensure the beam moves radially away from the foil, at which point ϕ_s is reduced to zero over a period of 0.5 ms (Fig. 2). The bunch circulates in the stationary bucket thereafter. The $(-\pi, \pi)$ phase limits are set by the zero crossing times of the RF waveform. For each turn, the symmetry point is found by finding the phase ϕ_1 which minimises Δ defined by

$$\Delta = \left| \sum_{\phi_1-\pi}^{\phi_1} f(\phi) - \sum_{\phi_1}^{\phi_1+\pi} f(\phi) \right|. \quad (7)$$

The symmetry point, expected to oscillate about the synchronous phase, is calculated to be around 122 degrees. This is close to the expected delay given that the bunch arrives at the monitor 4 cells (one third of the ring circumference) after the cavity.

RESULTS

In order to reconstruct the phase space, a number of turns of bunch monitor data corresponding to the small amplitude synchrotron period (~ 200 turns) is included. This is to ensure that the data covers at least half an oscillation, even at large amplitude. An example reconstruction, carried out for the first turn, in the stationary bucket case is shown in Fig. 3. We observe a high frequency component (at 47 MHz) and are investigating its source. With this in mind, the agreement between the data and the reconstruction is reasonable.

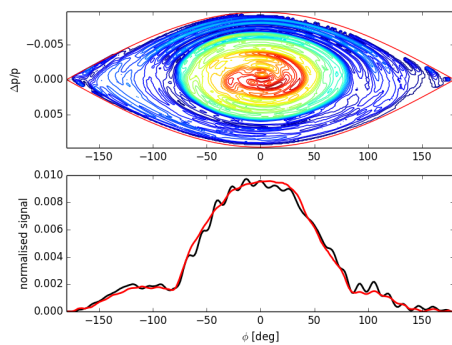


Figure 3: Top: Phase space reconstructed when the beam is in a stationary bucket. Bottom: a comparison of its projection (red) onto the phase axis with the data (black).

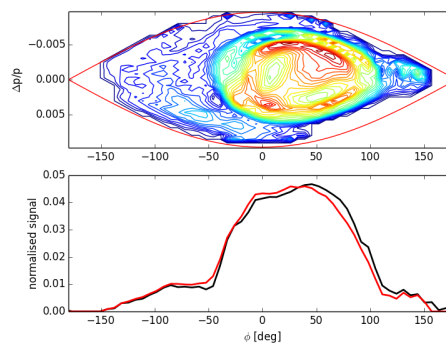


Figure 5: Phase space reconstruction and profile comparison immediately after a 40 degree phase jump is applied.

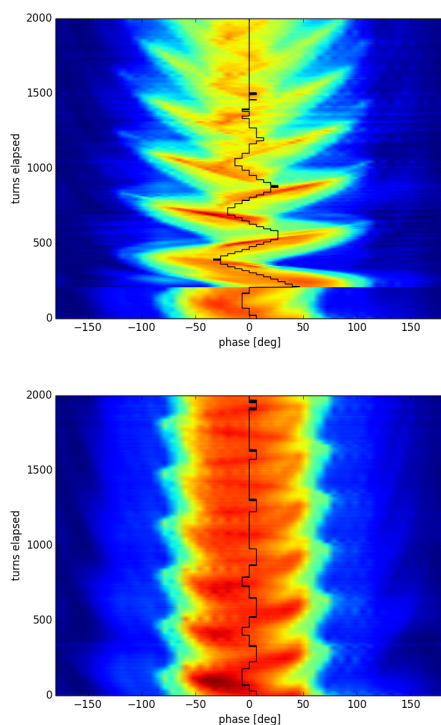


Figure 4: Bunch monitor data in the case where (top) a 40 degree phase jump in the rf waveform is applied at turn 207 and (bottom) no phase shift is applied. The time interval is shown in Fig. 2. The black line shows the turn-by-turn symmetry point in the data.

In a further test of the tomography reconstruction, an instantaneous phase jump was applied during the flat-top phase. This was repeated for a range of phase jumps in the positive and negative directions. In the example shown in Fig. 4, the applied jump is 40 degrees. The symmetry point of the bunch monitor data, immediately after the jump, shows an initial shift in agreement with this. Thereafter the symmetry point follows a damped oscillation around the synchronous phase — the damping is an expected effect of decoherence. This is borne out by comparing the tomography reconstruction

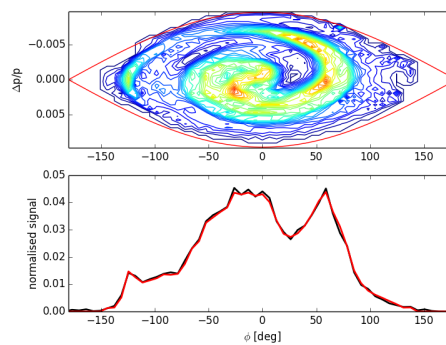


Figure 6: Phase space reconstruction and profile comparison about 1000 turns after a 40 degree phase jump is applied.

tions immediately after the phase jump (Fig. 5) and around three synchrotron oscillations later (Fig. 6). In the first case, the distribution is seen to be shifted to the right by about the expected amount, whereas in the latter case filamentation resulting from decoherence is clearly in evidence.

DISCUSSION

It has been shown that the existing synchrotron tomography code can reconstruct the longitudinal phase space in a scaling FFA. Some improvements are required so that approximations are avoided to allow more general cases to be treated. For example, the turn-by-turn revolution frequency should be correctly specified by taking into account the varying machine radius. To accommodate the flexible RF programme, parameters such as V_{rf} and ϕ_s should also be free to vary turn-by-turn. In addition, higher harmonics in the RF waveform produced by the broadband RF cavities should be included in the tracking (the existing code is limited to dual-harmonic RF). A more general code that includes these features is currently under development.

REFERENCES

- [1] L. Michelotti, “Integral for longitudinal phase space tomography on equilibrium distributions”, *Phys. Rev. ST Accel Beams*, vol. 6, p. 024001, 2003.

- Content from this work may be used under the terms of the CC BY 3.0 licence (© 2019). Any distribution of this work must maintain attribution to the author(s), title of the work, publisher, and DOI
- [2] S. Hancock, M. Lindroos and S. Koscielniak, “Longitudinal phase space tomography with space charge”, *Phys. Rev. ST Accel Beams*, vol. 3, p. 124202, 2000.
- [3] CERN tomography code, <http://cern.ch/tomography>
- [4] C. Montag *et al.*, “Tomographic phase space reconstruction during rebucketing in the Relativistic Heavy Ion Collider”, *Phys. Rev. ST Accel Beams*, vol. 5, p. 082801, 2002.
- [5] D. J. Adams *et al.*, “Beam Loss Studies of the ISIS Synchrotron Using ORBIT”, in *Proc. 3rd Int. Particle Accelerator Conf. (IPAC'12)*, New Orleans, LA, USA, May 2012, paper TH-PPP088, pp. 3942–3944.
- [6] N. J. Evans, S. E. Kopp, P. Adamson, and D. J. Scott, “A New Tool for Longitudinal Tomography in Fermilab’s Main Injector and Recycler Rings”, in *Proc. 4th Int. Particle Accelerator Conf. (IPAC'13)*, Shanghai, China, May 2013, paper MOPWA061, pp. 816–818.
- [7] M. Yoshimoto *et al.*, “Measurement of Momentum Spread of the Injection Beam with Longitudinal Tomography Method in the J-PARC RCS”, in *Proc. 6th Int. Particle Accelerator Conf. (IPAC'15)*, Richmond, VA, USA, May 2015, pp. 944–946. doi:10.18429/JACoW-IPAC2015-MOPTY003
- [8] K. R. Symon *et al.*, “Fixed-field alternating-gradient particle accelerators”, *Phys. Rev.*, vol. 103 no. 6, p. 1837, 1956.
- [9] S. L. Sheehy *et al.*, “Characterization techniques for fixed-field alternating gradient accelerators and beam studies using the KURRI 150 MeV proton FFAG”, *Prog. Theor. Exp. Phys.*, vol. 7, p. 073G01, 2016.
- [10] Y. Ishi *et al.*, “Present Status and Future of FFAGs at KURRI and the First ADSR Experiment”, in *Proc. 1st Int. Particle Accelerator Conf. (IPAC'10)*, Kyoto, Japan, May 2010, paper TUOCRA03, pp. 1327–1329.